Potential Mechanism of the Anti-trypanosomal Activity of Organoruthenium Complexes with Bioactive Thiosemicarbazones

**Bruno Demoro · Miriam Rossi · Francesco Caruso ·
Daniel Liebowitz · Claudio Olea-Azar ·
Ulrike Kemmerling · Juan Diego Maya · Helena Guiset ·
Virtudes Moreno · Chiara Pizzo · Graciela Mahler ·
Lucía Otero · Dinorah Gambino**

Abstract In the search for new metal-based drugs against diseases produced by trypanosomatid parasites, four organoruthenium(II) compounds $[Ru_2(p\text{-cymene})_2(L)_2]X_2$, where L are bioactive 5-nitrofuryl-containing thiosemicarbazones and X=Cl or PF_6, had been previously obtained. These compounds had shown activity on *Trypanosoma brucei*, the etiological agent of African trypanosomiasis. Because of genomic similarities between trypanosomatides, these ruthenium compounds were evaluated, in the current work, on *Trypanosoma cruzi*, the parasite responsible of American trypanosomiasis (Chagas disease). Two of them showed significant in vitro growth inhibition activity against the infective trypomastigote form of *T. cruzi* (Dm28c clone, $IC_{50}=11.69$ and 59.42 μM for $[Ru_2(p\text{-cymene})_2(L4)_2]Cl_2$ and $[Ru_2(p\text{-cymene})_2(L1)_2]Cl_2$, respectively, where HL4=5-nitrofuryl-*N*-phenylthiosemicarbazone and HL1=5-nitrofurylthiosemicarbazone), showing fairly good selectivities toward trypanosomes with respect to mammalian cells (J774 murine macrophages). Moreover, $[Ru_2(p\text{-cymene})_2(L2)_2]Cl_2$, where HL2=5-nitrofuryl-*N*-methylthiosemicarbazone, was synthesized in order to evaluate the effect of improved solubility on biological behavior. This new chloride salt showed higher activity against *T. cruzi* than that of the previously synthesized hexafluorophosphate one (Dm28c clone, $IC_{50}=14.30$ μM for the former and 231.3 μM for the latter). In addition, the mode of antitrypanosomal action of the organoruthenium compounds

B. Demoro · L. Otero (✉) · D. Gambino (✉)
Cátedra de Química Inorgánica, Departamento Estrella Campos,
Facultad de Química, Universidad de la República (UdelaR),
Gral. Flores 2124, 11800 Montevideo, Uruguay
e-mail: luotero@fq.edu.uy
e-mail: dgambino@fq.edu.uy

M. Rossi · D. Liebowitz
Department of Chemistry, Vassar College, Poughkeepsie,
NY 12604-0484, USA

F. Caruso
Istituto di Chimica Biomolecolare, Consiglio Nazionale delle
Ricerche, c/o Università di Roma La Sapienza,
Vecchio Istituto Chimico, Ple. Aldo Moro 5, 00185 Rome,
Italy

C. Olea-Azar
Departamento de Química Inorgánica y Analítica,
Facultad de Ciencias Químicas y Farmacéuticas,
Universidad de Chile, Casilla 233, Santiago, Chile

U. Kemmerling
Programa de Anatomía y Biología del Desarrollo,
ICBM, Facultad de Medicina, Universidad de Chile,
Independencia 1027, Santiago, Chile

J. D. Maya
Programa de Farmacología Molecular y Clínica, ICBM,
Facultad de Medicina, Universidad de Chile, Independencia 1027,
Santiago, Chile

H. Guiset · V. Moreno
Departamento de Química Inorgánica, Universitat Barcelona,
Martí i Franquès 1-11, 08028 Barcelona, Spain

C. Pizzo · G. Mahler
Cátedra de Química Farmacéutica, Departamento de Química
Orgánica, Facultad de Química, Universidad de la República
(UdelaR), Gral. Flores 2124, 11800 Montevideo, Uruguay

was investigated. The complexes were not only able to generate toxic free radicals through bioreduction but they also interacted with two further potential parasite targets: DNA and cruzipain, a cysteine protease which plays a fundamental role in the biological cycle of these parasites. The results suggest a "multi-target" mechanism of trypanosomicidal action for the obtained complexes.

Keywords Ruthenium *p*-cymene compounds ·
5-Nitrofuryl-containing thiosemicarbazones · American trypanosomiasis · Chagas disease · *Trypanosoma cruzi* · Mechanism of trypanosomicidal action

Introduction

Tropical parasitic diseases constitute a major health problem. Those produced by protozoa that belong to the trypanosomatid genus and kinetoplastid order, mainly Chagas disease (American trypanosomiasis, caused by *Trypanosoma cruzi*), human African trypanosomiasis (caused by *Trypanosoma brucei*), and leishmaniasis, account for the highest number of deaths among those illnesses designated by World Health Organization as neglected tropical diseases. One of the main current challenges related to these diseases is the discovery of new efficient drugs to cure and/or significantly improve the prognosis of the millions of people that are infected [1–5].

The development of broad-spectrum drugs active against multiple protozoa could offer an innovative and less expensive approach for anti-parasitic drug discovery [6]. This approach involves the recognition of common targets present in different parasites and of chemical scaffolds that could affect these targets. Recently, the genomas of *T. cruzi*, *T. brucei*, and *Leishmania major* have been decoded, showing a high degree of similarity [7]. Thus, clinically useful drugs affecting common enzymatic targets or metabolic pathways in the different trypanosomatid parasites are being sought [3]. In this sense, we are currently involved in the recognition of metal-based moieties that could inhibit either *T. cruzi* or *T. brucei* growth by acting on common targets.
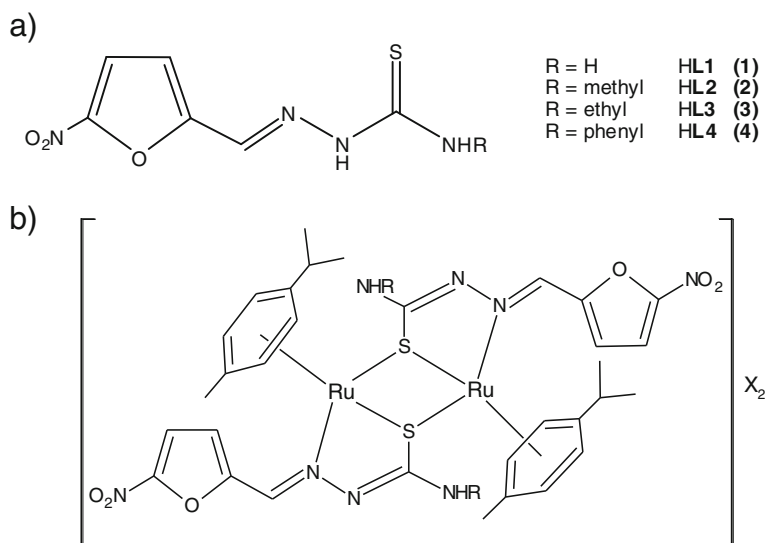
Different attempts toward the development of trypanosomicidal metal-based compounds have been described [8–12]. In particular, we have been working on the development of potential anti-trypanosomal metal-based agents through different strategies [1]. One of these approaches involves metal coordination of trypanosomicidal ligands. The design of anti-parasitic compounds which combine ligands bearing anti-trypanosomal activity and pharmacologically active metals in a single chemical entity could provide drugs

capable of modulating multiple targets simultaneously [13]. This strategy aims to enhance the efficacy and/or improve safety relative to drugs that address only a single target. In particular, we used this approach to develop classic Pd(II), Pt(II), Ru(II), and Ru(III) coordination compounds with bioactive 5-nitrofuryl-containing thiosemicarbazones as ligands. Most of these compounds had shown higher in vitro activity against *T. cruzi* than the reference anti-trypanosomal drug nifurtimox [14–17].

Although organoruthenium compounds had been previously identified as potential antimalarial agents, bioorganometallic compounds against trypanosomiasis have been less explored [18]. In the search for new metal-based antitrypanosomal agents, we have recently expanded our previous work on classical coordination complexes through the development of four organoruthenium compounds $[Ru^{II}_2(\eta^6\text{-}p\text{-}cymene)_2(L)_2]^{2+}$, including the bioactive 5-nitrofuryl-containing thiosemicarbazones L**1**–**4** as co-ligands (Fig. 1) [19]. Two of these complexes have shown significant in vitro growth inhibition activity against *T. brucei brucei*, a suitable model of the species that causes human African trypanosomiasis, and they were highly selective toward trypanosomal cells with respect to mammalian ones [19].

Taking into account the genomic analogies between *T. brucei* and *T. cruzi* and the previously observed anti-*T. cruzi* activity shown by the thiosemicarbazone ligands, in this work, the effects of these recently synthesized organoruthenium compounds on *T. cruzi* were explored. Moreover, the new chloride salt of $[Ru_2$ $(p\text{-}cymene)_2(L2)_2]^{2+}$ complex, where H**L2**=5-nitrofuryl-*N*-methylthiosemicarbazone, was synthesized in order to evaluate the effect of improving solubility (by changing the counter anion from hexafluorophosphate to chloride) on its biological effect. Its crystal structure was solved using single-crystal X-ray diffraction methods. Different targets were investigated in order to gain insight into the probable mechanism of the trypanosomicidal action of these organoruthenium compounds: redox metabolism (ROS generation), DNA, and cruzipain. The main mode of action of the 5-nitrofuryl-containing thiosemicarbazone co-ligands, which is expected to remain in the ruthenium compounds, involves the intracellular reduction of the nitro moiety followed by redox cycling, yielding reactive oxygen species (ROS) known to cause parasite damage [20]. On the other hand, cruzipain, the main *T. cruzi* cysteine protease, has been validated as a drug target; certain compounds that include the thiosemicarbazone moiety have shown inhibitory effects on this enzyme's activity [21, 22]. Additionally, DNA is a recognized parasite target, and Ru–arene compounds have shown the ability to interact with DNA through different mechanisms inducing permanent distorsions of this biomolecule [23–25].

Fig. 1 **a** Bioactive 5-nitrofuryl-containing thiosemicarbazones (*HL*) selected as co-ligands (compounds **1–4**). **b** [Ru$^{II}_2$(η^6-*p*-cymene)$_2$(L)$_2$]X$_2$ complexes **5–8**: [Ru$^{II}_2$(η^6-*p*-cymene)$_2$(**L1**)$_2$]Cl$_2$ (**5**), [Ru$^{II}_2$ (η^6-*p*-cymene)$_2$(**L2**)$_2$](PF$_6$)$_2$ (**6**), [Ru$^{II}_2$(η^6-*p*-cymene)$_2$(**L3**)$_2$](PF$_6$)$_2$ (**7**), and [Ru$^{II}_2$(η^6-*p*-cymene)$_2$ (**L4**)$_2$]Cl$_2$ (**8**) [19]

a)

R = H   H**L1** (**1**)
R = methyl   H**L2** (**2**)
R = ethyl   H**L3** (**3**)
R = phenyl   H**L4** (**4**)

b)

Results and discussion

Chemistry

Synthesis and characterization of [Ru$_2$(p-cymene)$_2$(L2)$_2$]Cl$_2$ (9)

The chloride salt of [Ru$_2$(*p*-cymene)$_2$(**L2**)$_2$]$^{2+}$ was synthesized with high purity and a reasonable yield. Analytical and Fourier transform infrared (FTIR) spectroscopic results are in agreement with the proposed formula. The ESI-MS, infrared, and ^{1}H NMR spectroscopic results are in agreement with those previously reported for [Ru$_2$(*p*-cymene)$_2$(**L2**)$_2$](PF$_6$)$_2$ [19, 26].

Crystal structure of [Ru$_2$(p-cymene)$_2$(L2)$_2$]Cl$_2$·2H$_2$O

Figure 2 depicts the molecular structure of complex [Ru$_2$ (*p*-cymene)$_2$(**L2**)$_2$]Cl$_2$·2H$_2$O consisting of a binuclear dicationic complex. A central core formed by two Ru and two S atoms is observed. A two fold axis passes at the center of the Ru–S–Ru–S four-membered ring, and so the asymmetric unit contains half the molecule. Each ruthenium atom, in a pseudo-octahedral geometry, is η^6-coordinated to a *p*-cymene ring (occupying three coordination positions), one N and two S atoms leading to a typical three-legged piano stool structure (Table 1) [27].
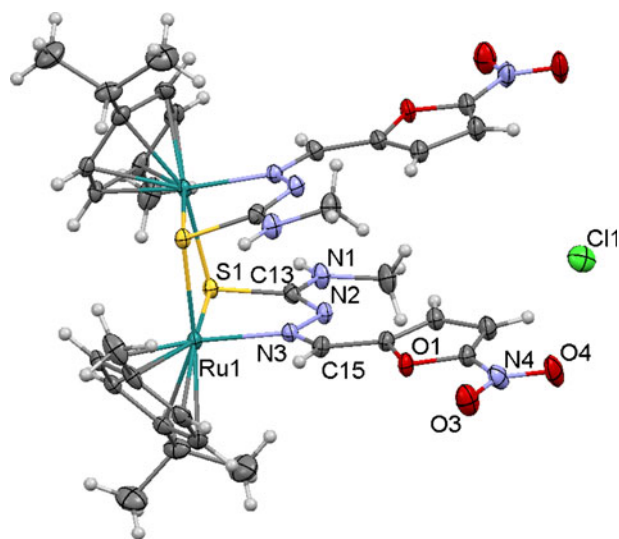
The five-membered ring [Ru1-N2-N1-C13-S1-(Ru1)] shows good planarity as the distances from its least-square plane and its corresponding atoms are within 0.08 Å. The dihedral angle between this plane and its equivalent [Ru1'-N2'-N1'-C13'-S1'-(Ru1')] is 18.2°, whereas that between [Ru1-N2-N1-C13-S1-(Ru1)] and that formed by Ru1-S1-Ru1'-S1' is 80.9°. The dihedral angle between [Ru1-N2-N1-C13-S1-(Ru1)] and the furyl ring is 6.8° and that between the

furyl and its attached nitro group is 1.8°, suggesting an overall flat arrangement for the **L2** ligand.

The molecular structure of the title compound resembles two recent structures described by us [19], where the *N*-methyl terminal group present in ligand **L2** was replaced by NH (**L1** in Table 1) or *N*-ethyl (**L3** in Table 1) moieties. No significant differences in bond distances and angles are observed.

Biological studies

The ruthenium compounds under study are very soluble in DMSO, and the presence of 1–2 % DMSO proved to be enough for their dissolution in the aqueous media needed for

Fig. 2 Molecular structure of [Ru$_2$(*p*-cymene)$_2$(**L2**)$_2$]Cl$_2$·2H$_2$O (**9**). Labels are limited to the asymmetric unit. H and some C atoms are not labeled. H (hydrate) could not be located in the Fourier map, so its O atom is omitted in this picture; only one Cl anion is shown

Table 1 Selected geometrical parameters including bond distances, separation for non-bonded atoms, dihedral angles, and bond angles for [Ru$_2$(*p*-cymene)$_2$(**L2**)$_2$]Cl$_2$ (**9**), [Ru$_2$(*p*-cymene)$_2$(**L1**)$_2$]Cl$_2$ (**5**) [20], and [Ru$_2$(*p*-cymene)$_2$(**L3**)$_2$](PF$_6$)$_2$ (**7**) complexes [19]

	[Ru$_2$(*p*-cymene)$_2$(**L2**)$_2$]Cl$_2$ (**9**)	[Ru$_2$(*p*-cymene)$_2$(**L1**)$_2$]Cl$_2$ (**5**)	[Ru$_2$(*p*-cymene)$_2$(**L3**)$_2$](PF$_6$)$_2$ (**7**)
Ru1–Ru2	3.5304(3)	3.565(1), [3.537(1)]	3.557(1)
Ru1–S1, Ru1–S2	2.4237(7), 2.3475(6)	2.350(1), 2.428(2) (Ru3) [2.344(2), 2.417(2)]	2.3521(15), 2.4313(16)
Ru2–S1, Ru2–S2	2.4237(7), 2.3475(6)	2.418(2), 2.347(2) (Ru4) [2.420(2), 2.349(1)]	2.3495(15), 2.4009(16)
Ru–N	2.088(2), 2.088(2)	2.077(5), 2.077(5) (Ru3) [2.081(5), 2.093(5)] (Ru4)	2.085(4), 2.092(4)
Ru–C(aromatic), range	2.193(3), 2.251(3)	2.162(9)–2.275(5)	2.178(5)–2.277(5)
Ru–arene centroid	1.702(3)	1.701(7), 1.707(7) (Ru3) [1.719(7) 1.706(7)] (Ru4)	1.711(6), 1.705(6)
N′–N″ stacking	3.314(4)	3.285(9), [3.387(8)]	3.401(6)
S2–Ru–N	80.7	80.6, [80.5]	80.8
S1–Ru–S2	84.0	83.5, [82.5]	82.4
S1–Ru–N	90.8	88.9, [89.4]	90.3
centroid–Ru–S1	128.6	130.4, [129.0]	128.5
centroid–Ru–S2	125.4	126.8, [128.0]	126.2
centroid–Ru–N	131.5	130.7, [130.2]	131.5
Ru1–S1–S2 dihedral, Ru2–S1–S2	10.7	14.0, [12.1]	12.7
Furyl–furyl dihedral	4.6	7.5, [13.7]	13.9(2)

Distances in angstrom; angles in degrees. Values in square brackets are a selection of geometrical data for the second molecule in the asymmetric unit of [Ru$_2$(*p*-cymene)$_2$(**L1**)$_2$]Cl$_2$; for instance, Ru3–Ru4 separation of 3.537(1) Å is shown next to that of Ru1–Ru2

the biological tests. The stability of all complexes in 2 % DMSO/98 % pH 7.4 phosphate buffer was stated over time by UV/vis spectroscopy at room temperature. It was previously reported that the compounds exhibit in this medium one absorption band in the UV range (λ_{max} in the 287 to 311 nm region depending on the compound) and a broad band in the visible range (λ_{max} in the 413 to 426 nm region) [19]. No changes could be observed in the spectra within 24 h. The existence of the dimeric species in solution was previously stated by ESI-MS for at least 24 h [19].

In vitro anti T. cruzi activity on epimastigotes

Previously obtained ruthenium compounds [19] were evaluated in this work for their anti *T. cruzi* activities against epimastigotes of *T. cruzi* (Dm28c strain) as a first screening. **L1**–**L3** ruthenium compounds (**5**–**7**) showed IC$_{50}$ values higher than 100 μM. Only [Ru$_2$(*p*-cymene)$_2$(**L4**)$_2$]Cl$_2$ (**8**) showed moderate activity (86.10±14.11 μM), but lower than that of the free thiosemicarbazone ligand (Table 2).

Viability on T. cruzi (Dm28c strain and Y strain) trypomastigotes

The effect of compounds **5**–**8** on the trypomastigote form of Y strain and the Dm28c clone of the parasite was evaluated. The results are presented in Table 2.

It is known that the activity against one form of the parasite life cycle does not guarantee similar activity against the other forms. To explain this fact, it is necessary to consider the morphologic changes that occur during transformation between forms along the biological cycle of the parasite, which imply important metabolic and macromolecular content changes that alter sensitivity to drugs. The assayed compounds were significantly more active against the trypomastigote form of *T. cruzi* than against the epimastigote form (Mann–Whitney non-parametric test: $p > 0.0001$). These results are significant since epimastigotes are present in the gut of the insect vector, but trypomastigotes are the infective forms in the mammalian host.

Among the previously reported ruthenium compounds, **5** and **8** showed significant in vitro growth inhibition activity against the trypomastigote form of *T. cruzi* (Mann–Whitney non-parametric test: $p > 0.0001$). The same two compounds showed fairly good selectivity toward trypanosomal cells with respect to mammalian cells (J774 murine macrophages; Table 2). [Ru$_2$(*p*-cymene)$_2$(**L4**)$_2$]Cl$_2$ (**8**) was the most active compound against trypomastigotes, and its activity was higher than that of the corresponding thiosemicarbazone ligand and the reference drug nifurtimox (IC$_{50}$=20.0 μM on Y strain trypomastigotes and 24.7 μM on Dm28c clone trypomastigotes).

Both originally developed chloride salts of [Ru$_2$(*p*-cymene)$_2$(L)$_2$]$^{2+}$ were more active than the hexafluorophosphate

Table 2 In vitro activity against *T. cruzi* epimastigotes and trypomastigotes of two strains: Y and Dm28c clone and cytotoxicity on murine macrophages of the Ru-*p*-cymene derivatives

Compound	IC$_{50}$/μM macrophages	*T. cruzi*		
		IC$_{50}$/μM Y strain (*tryp*)	IC$_{50}$/μM Dm28c (*tryp*)	IC$_{50}$/μM Dm28c (*epi*)
5, [Ru$_2$(*p*-cymene)$_2$(**L1**)$_2$]Cl$_2$	>100 [19]	59.42±1.12	116.9±1.085	>100
6, [Ru$_2$(*p*-cymene)$_2$(**L2**)$_2$](PF$_6$)$_2$	ND	193.4±1.13	231.3±1.108	>100
9, [Ru$_2$(*p*-cymene)$_2$(**L2**)$_2$]Cl$_2$	ND	75.96±1.10	14.30±1.065	ND
7, [Ru$_2$(*p*-cymene)$_2$(**L3**)$_2$](PF$_6$)$_2$	ND	87.21±1.06	130.9±1.051	>100
8, [Ru$_2$(*p*-cymene)$_2$(**L4**)$_2$]Cl$_2$	26.2±1.7 [19]	11.69±1.08	8.681±1.008	86.10±14.11[b]
1, H**L1**	64.8±8.7 [19]	ND	9.76±1.47	11.77±2.91[b]
2, H**L2**	36.4±4.2[a]	ND	17.38±1.98	11.87±1.66[b]
3, H**L3**	34.0±2.1[a]	ND	18.48±1.71	15.88±2.83[b]
4, H**L4**	>100[a]	ND	22.72±1.64	9.52±1.59[b]
[Ru(*p*-cymene)Cl$_2$]$_2$	ND	ND	63.67±2.64	>100[b]

Results for the free ligands and the precursor [Ru(*p*-cymene)Cl$_2$]$_2$ are included for comparison. Results are the means of three different experiments with SE values

ND not determined, *tryp* trypomastigote form of *T. cruzi*, *epi* epimastigote form of *T. cruzi*

[a] Significant differences between macrophages and trypomastigotes Dm28c strain ($p<0.001$)

[b] Significant difference between trypomastigotes and epimastigotes Dm28c strain ($p<0.001$)

ones (Table 2). Differences in solubility could explain the large and unexpected differences in the anti-trypanosomal activity of this series of structurally related compounds. To test this hypothesis, [Ru$_2$(*p*-cymene)$_2$(**L2**)$_2$]Cl$_2$ (**9**) was synthesized and evaluated. This compound showed a 2- to 17-fold higher activity (Y strain IC$_{50}$=75.96 μM; Dm28c clone IC$_{50}$=14.30 μM) than the less soluble compound **6**, [Ru$_2$(*p*-cymene)$_2$(**L2**)$_2$](PF$_6$)$_2$ (Table 2).

It had been previously reported that compounds **5**, [Ru$_2$(*p*-cymene)$_2$(**L1**)$_2$]Cl$_2$, and **8**, [Ru$_2$(*p*-cymene)$_2$(**L4**)$_2$]Cl$_2$, are also the most active compounds against *T. brucei brucei*. This fact would validate our proposal of the development of broad-spectrum drugs active against multiple trypanosomatid protozoa as a potentially innovative approach for anti-parasitic drug discovery.

Mechanism of action

The organoruthenium compounds were designed to show a dual or even a multiple mechanism of action by affecting different targets or biologically significant processes in the parasite. They could act by the generation of intra-parasite toxic free radicals through the 5-nitrofuryl moiety and/or by inhibition of cruzipain through the thiosemicarbazone pharmacophore. Additionally, they could interact with DNA mainly through the Ru–arene moiety. Accordingly, different studies were performed in order to validate the proposed targets and to get insight into the probable mechanism of action of the new Ru-*p*-cymene compounds.

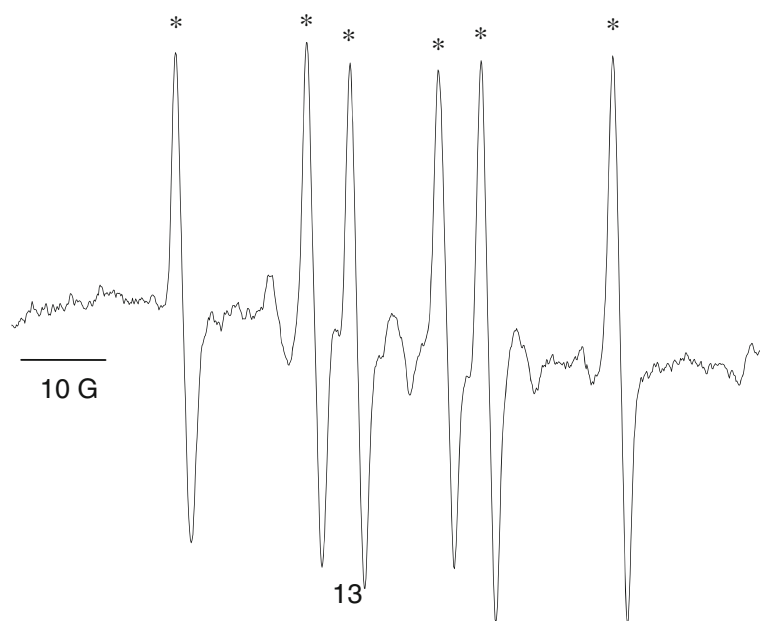*Capacity of the derivatives to generate free radical species into T. cruzi*

The proposed bioreduction of the 5-nitrofuryl-containing thiosemicarbazone ligands and their metal complexes involves the production of toxic free radical species in the parasite. The free radical production capacity of the organoruthenium compounds was assessed using electron paramagnetic resonance (EPR) incubating the Ru-*p*-cymene compounds with intact *T. cruzi* (Dm28c strain) epimastigotes. In order to detect possible intracellular free radical species having short half-lives, 5,5-dimethyl-1-pyrroline-*N*-oxide (DMPO) was added as a spin trapping agent. The EPR spectrum for **7**, [Ru$_2$(*p*-cymene)$_2$(**L3**)$_2$](PF$_6$)$_2$, is shown in Fig. 3. The obtained splitting pattern and the corresponding hyperfine constants (a_N=15.0 G, a_H=22.5 G) are in agreement with the trapping of a carbon-centered radical by DMPO [28, 29]. This spin adduct could be related to the bioreduction of the complexes and the formation of a DMPO–nitroheterocyclic radical species. This adduct was detected for all the studied complexes. In addition, intracellular hydroxyl radical species was also observed at the beginning of the experiments (results not shown), but only the DMPO–nitrocompound adduct stabilizes during several minutes.

Even though all the compounds were capable of producing free radicals in the intact parasite, no correlation could be observed between the intensity of the EPR signals and the observed anti *T. cruzi* activity. In this sense, obtained ruthenium compounds maintain the mode of action of the free thiosemicarbazone ligand including the 5-nitrofuryl pharmacophore [32], but it does not seem to be their main mechanism of trypanosomicidal action.

Fig. 3 EPR spectrum obtained after 5 min incubation of **7**, [Ru$_2$(p-cymene)$_2$(**L3**)$_2$](PF$_6$)$_2$, (1 mM) with intact *T. cruzi* epimastigotes (Dm28c strain; final protein concentration, 4–8 mg/mL), NADPH (1 mM), and DMPO (100 mM). *Characteristic signals of DMPO–nitrocompound spin adduct. Not assigned signals correspond to DMPO degradation; they were also observed in the absence of any metal complex [30, 31]

DNA interaction studies

In order to gain insight into DNA interaction mechanism, the compounds were tested on plasmid DNA using atomic force microscopy (AFM) and on CT DNA using DNA viscosity measurements. In this sense, it should be noted that the covalent interaction of these complexes with DNA does not seem to be possible due to the lack of labile bonds like Ru–Cl, as has been previously stated [19].

AFM and viscosity measurements results AFM has been proven to be a useful tool for imaging DNA and also DNA interactions with metal complexes [33, 34]. In this sense, organoruthenium complexes were incubated with pBR322 plasmid DNA. AFM images are depicted in Fig. 4. All complexes modified the tertiary structure of the plasmid; this is visualized as changes in the shape of DNA, like kinks, cross-linking, and supercoiling. The observed effect is slightly affected by the nature of the thiosemicarbazone ligand. However, **8**, [Ru$_2$(p-cymene)$_2$(**L4**)$_2$]Cl$_2$, seems to show the most evident interaction among the four new Ru-p-cymene compounds. For instance, its effect could be visualized as more intense modifications of DNA tertiary structure together with an increase of DNA thickness (see Fig. 4).

Viscosity measurements

Trying to elucidate the binding mode of the ruthenium compounds under study, viscosity measurements for increasing r_i values were carried out on CT DNA. The results are shown for compound **5**, [Ru$_2$(p-cymene)$_2$(**L1**)$_2$](Cl)$_2$, in Fig. 5. All the complexes increased the viscosity of CT DNA solutions in a concentration-dependent manner in the tested r_i values. This behavior is usually attributed to intercalators as base pairs are separated to accommodate the binding ligand, leading to an increase of DNA length with a concomitant rise in viscosity [35–37]. Nevertheless, exhaustive studies performed on other ruthenium(II)–arene compounds had shown important distortional effects on DNA, but discarded intercalation on double helical DNA through the arene moiety for p-cymene and benzene ruthenium complexes [38]. Other types of noncovalent interactions, like hydrogen bonding, van der Waals, hydrophobic contacts, and electrostatic interactions, could be responsible for the observed effects [39].
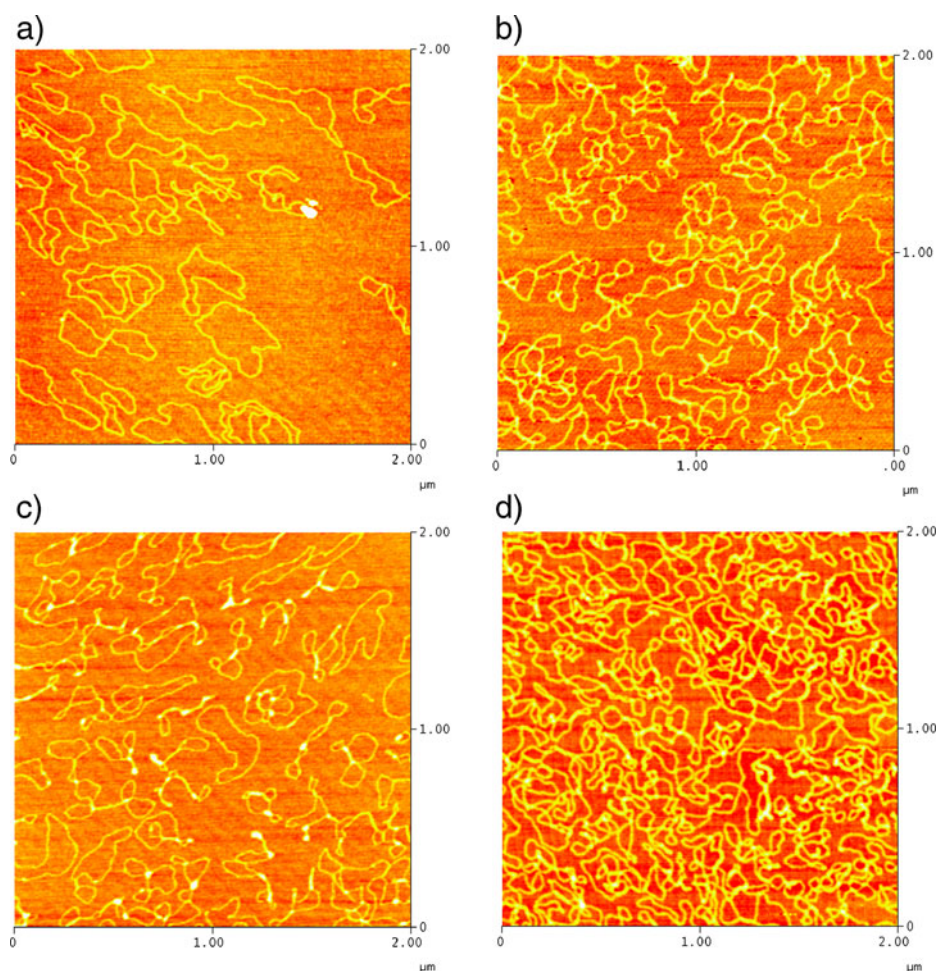
Cruzipain inhibitory activity

The ruthenium compounds were screened against cruzipain enzyme at 10 and 50 µM inhibitor concentrations. According to the results shown in Table 3, these compounds have low to moderate potency as cruzipain inhibitors. Compounds **8** and **6** have the best inhibitory effect: 94 and 83 % at 50 µM, respectively. Further studies are needed to determine a structure–activity relationship for these compounds.
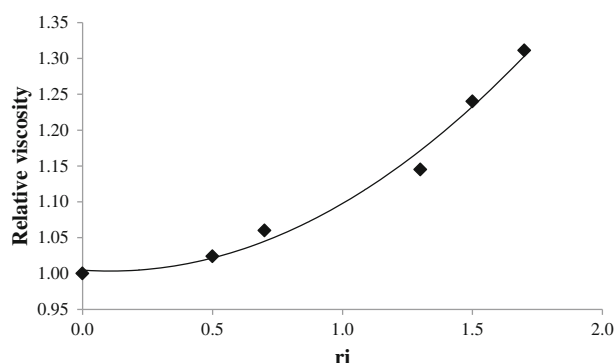
Conclusions

Dimeric ruthenium-p-cymene compounds with bioactive nitrofuryl-containing thiosemicarbazones (L)**1**–**4** as co-ligands with the formula [Ru$_2$(p-cymene)$_2$(L)$_2$]X$_2$, where X=Cl or PF$_6$, were evaluated on *T. cruzi*. All choride salts of the complexes showed in vitro activity against the infective trypomastigote form of *T. cruzi*, and compounds **8**, [Ru$_2$(p-cymene)$_2$(**L4**)$_2$]Cl$_2$, and **9**, [Ru$_2$(p-cymene)$_2$(**L2**)$_2$]Cl$_2$, were

Fig. 4 AFM images showing the modifications suffered by pBR322 DNA due to interaction with the Ru/*p*-cymene compounds: **5**, [Ru$_2$(*p*-cymene)$_2$(**L1**)$_2$]Cl$_2$ (**a**), **6**, [Ru$_2$(*p*-cymene)$_2$(**L2**)$_2$](PF$_6$)$_2$ (**b**), **7**, [Ru$_2$(*p*-cymene)$_2$(**L3**)$_2$](PF$_6$)$_2$ (**c**), **8**, [Ru$_2$(*p*-cymene)$_2$(**L4**)$_2$]Cl$_2$ (**d**) for molar ratio compound: DNA base pairs 1:5 and 24 h incubation at 37 °C

more active than the reference tripanocidal drug nifurtimox. The complexes that show activity against *T. cruzi* have previously shown high activities against *T. brucei brucei*. These results seem to validate the proposed strategy: the development of potential metal-based drugs against both parasites. This approach must be further investigated in the near future.

Fig. 5 Relative viscosity vs. r_i curve for compound **5**, [Ru$_2$(*p*-cymene)$_2$(**L1**)$_2$](Cl)$_2$ (r_i=mole of complex/mole of DNA base pairs)

Experiments performed to get insight into the probable mechanism of trypanosomicidal activity showed that all the complexes generate toxic free radicals by bioreduction in the parasite, interact with DNA, and show a low to moderate inhibition of cruzipain, the cystein protease which plays a fundamental role in the biological cycle of the parasite. Nevertheless, the extent of these effects seems not to clearly correlate with the observed biological activity. Therefore, these results do not allow to ascertain the main target of the compounds, suggesting the possibility of a combined

Table 3 Biological activity of the Ru compounds on cruzipain

Compound	CI (%)[a] at 10 μM	CI (%)[a] at 50 μM
5, [Ru$_2$(*p*-cymene)$_2$(**L1**)$_2$]Cl$_2$	19±9	69±1
6, [Ru$_2$(*p*-cymene)$_2$(**L2**)$_2$](PF$_6$)$_2$	59±4	83±1
7, [Ru$_2$(*p*-cymene)$_2$(**L3**)$_2$](PF$_6$)$_2$	33±1	78±2
8, [Ru$_2$(*p*-cymene)$_2$(**L4**)$_2$]Cl$_2$	29±8	94±1

Values are means of two values

[a] CI=percent of cruzipain inhibition

"multiple-target" mechanism. In fact, other potential targets could not be discarded.

This work on organometallic ruthenium compounds could be considered a contribution for further oganometallic antitrypanosomal drug development.

Experimental

All common laboratory chemicals were purchased from commercial sources and used without further purification. [Ru(p-cymene)Cl$_2$]$_2$ and the thiosemicarbazone ligands (Fig. 1a) were prepared according to previously published procedures [13, 20]. [Ru$^{II}_2$(η^6-p-cymene)$_2$(**L1**)$_2$]Cl$_2$ (**5**), [Ru$^{II}_2$(η^6-p-cymene)$_2$(**L2**)$_2$](PF$_6$)$_2$ (**6**), [Ru$^{II}_2$(η^6-p-cymene)$_2$(**L3**)$_2$](PF$_6$)$_2$ (**7**), and [Ru$^{II}_2$(η^6-p-cymene)$_2$(**L4**)$_2$]Cl$_2$ (**8**) were prepared and characterized as previously described [19].

Physicochemical characterization

C, H, and N analyses were performed with a Carlo Erba model EA1108 elemental analyzer. UV/vis spectra were recorded on a Shimadzu UV-1603 instrument. The FTIR spectra (4,000–400 cm^{-1}) of the complexes and the free ligands were measured as KBr pellets with a Bomen FTIR model MB102 instrument.

Synthesis of [Ru$^{II}_2$(η^6-p-cymene)$_2$(**L2**)$_2$]Cl$_2$ (**9**)

Solutions of [Ru(p-cymene)Cl$_2$]$_2$ (0.08 mmol, 50 mg; 10 mL MeOH) and HL2 (0.16 mmol, 38 mg; 10 mL MeOH) were mixed and stirred at room temperature for 24 h and were slowly evaporated to yield the dichloride compound. Yield was 23 mg (28 %). Anal (in percent) calculations for Ru$_2$Cl$_2$C$_{34}$H$_{42}$N$_8$O$_6$S$_2$: C, 41.01; H, 4.22; N, 11.25. Found: C, 40.96; H, 4.27; N, 11.16. FTIR (KBr)/cm^{-1}: ν(C=N) 1,588, ν_s(NO$_2$) 1351, ν(N–N) 1,168, δ(NO$_2$)+furan modes or furan hydrogen wagging symmetric modes 813. Suitable crystals for X-ray diffraction were obtained by slow evaporation of a methanolic solution.

X- ray crystallographic studies

Suitable crystals for X-ray diffraction data were obtained as described above. Data were collected at 125(2)K using graphite monochromated Mo Kα radiation in a Bruker SMART APEX II CCD X-ray diffractometer. Structure resolution and refinement were performed using SHELX [40]. Details are included in Table 4. Those H atoms not found in Fourier maps were calculated and constrained as riding on their bound atoms. The crystal structure has been deposited as CCDC 819344.

Table 4 Crystal data and structure refinement for **9**, [Ru$_2$(p-cymene)$_2$(**L2**)$_2$]Cl$_2$

	9, [Ru$_2$(p-cymene)$_2$(**L2**)$_2$]Cl$_2$·2H$_2$O
Empirical formula	C$_{34}$H$_{42}$Cl$_2$N$_8$O$_8$Ru$_2$S$_2$
Crystal color	Purple
Formula weight	1,029.94
Crystal system	Monoclinic
Space group	C2/c
Temperature (K)	125(2)
Wavelength (Å)	0.71073
a (Å)	20.9221(12)
b (Å)	12.2472(7)
c (Å)	17.0856(10)
β (deg)	108.254(1)
Volume (Å^3)	4,157.7(4)
Z, density (mg/mm^3)	4, 1.642
Absorption coefficient	1.013
Crystal size (mm)	0.29×0.25×0.24
θ range data collection	1.95, 28.70
Limiting indices	−28,28/−16, 16/−23, 22
Data collected/unique	20,103/5,375
Max (min) transmission	0.74 (0.79)
Refinement method	F^2
Refined data/parameters	4,582/261
Goodness of fit on F^2	1.008
Final R^a, Rw [I>2sigma(I)]	0.0365/ 0.1019

^{a} $R_1 = \Sigma ||F_o| - |F_c|| / \Sigma |F_o|$, $wR_2 = [\Sigma w(|F_o|^2 - |F_c|^2)^2 / \Sigma w(|F_o|^2)^2]^{1/2}$

Biological studies

Activity on Dm28c strain T. cruzi epimastigotes

T. cruzi epimastigotes Dm28c strain, from our own collection (Programa de Farmacología Molecular y Clínica, Facultad de Medicina, Universidad de Chile), were grown at 28 °C in Diamond's monophasic medium, as reported earlier but replacing blood by 4 μM hemin [41]. Heat-inactivated newborn calf serum was added to a final concentration of 4 %. Compounds dissolved in DMSO (1 % final concentration) were added to a suspension of 3×10^6 epimastigotes/mL. Parasite growth was followed with nephelometry. No toxic effect of DMSO alone was observed. From the epimastigote exponential growth curve, the culture growth constant (k) for each compound concentration and for controls was calculated (regression coefficient>0.9, p<0.05). This constant corresponds to the slope resulting from plotting the natural logarithm (Ln) of nephelometry lecture vs. time [42]. IC$_{50}$ is the drug concentration needed to reduce k in 50 %, and it was calculated using linear regression analysis from the k values and the concentrations used for the experiments. Reported values are the mean of at least three independent experiments.

Viability on *T. cruzi* (Dm28c strain and Y strain) trypomastigotes

Vero cells were infected with *T. cruzi* metacyclic trypomastigotes from 15-day-old Y strain or Dm28c clone epimastigote cultures. Subsequently, the trypomastigotes harvested from this culture were used to infect further Vero cell cultures at a density of 1×10^6 parasites per 25 cm². These trypomastigote-infected Vero cell cultures were incubated at 37 °C in humidified air and 5 % CO₂ for 5–7 days. After this time, the culture media were collected and centrifuged at $3,000 \times g$ for 5 min; the trypomastigote-containing pellets were resuspended in Roswell Park Memorial Institute Media (RPMI) supplemented with 5 % fetal bovine serum and penicillin–streptomycin at a final density of 1×10^7 parasites/mL. Trypomastigotes of 210×10^6 are equivalent to 1 mg of protein or 12 mg of wet weight. Viability assays were performed using the 3-(4,5-dimethylthiazol-2-yl)-2,5-diphenyl tetrazolium bromide (MTT) reduction method as previously described [43, 44]. Briefly, 1×10^7 trypomastigotes were incubated in fetal bovine serum–RPMI culture medium at 37 °C for 24 h with and without the Ru complexes under study at 5–100 μM final concentrations. An aliquot of the parasite suspension was extracted and incubated in a flat-bottom 96-well plate and MTT was added at a final concentration of 0.5 mg/mL, incubated at 28 °C for 4 h, and then solubilized with 10 % sodium dodecyl sulfate 0.1 mM HCl and incubated overnight. Formazan formation was measured at 570 nm with the reference wavelength at 690 nm in a multi-well reader (Labsystems Multiskan MS). Untreated parasites were used as negative controls (100 % of viability). Finally, a nonlinear regression analysis, using Log concentration vs. normalized response fit, with the GraphPad prism software was performed. Results are reported as IC_{50} values. Statistical significance was calculated using Mann–Whitney U test for non-parametric comparisons among the treatment groups.

Mechanism of action

Free radical production in *T. cruzi* (Dm28c strain)

The free radical production capacity of the new complexes was assessed in the parasite with ESR using DMPO for spin trapping. Each tested compound was dissolved in DMF (spectroscopy grade, approx. 1 mM) and the solution was added to a mixture containing the epimastigote form of *T. cruzi* (Dm28c strain; final protein concentration, 4–8 mg/mL) and DMPO (final concentration, 250 mM). The mixture was transferred to a 50-μL capillary. ESR spectra were recorded in the X band (9.85 GHz) using a Bruker ECS 106 spectrometer with a rectangular cavity and 50-kHz field modulation. All the spectra were registered in the same scale, after 15 scans [20].

DNA interaction studies

AFM studies To optimize the observation of the conformational changes in the tertiary structure of pBR322 plasmid DNA, the plasmid was heated at 60 °C for 30 min to obtain a majority of open circular form. Of the pBR322 DNA, 15 ng was incubated in an appropriate volume with the required compound concentration corresponding to the molar ratio base pairs (bp)/compound 5:1. Each ruthenium complex was dissolved in a minimal amount of DMSO and (4-(2-hydroxyethyl)-1-piperazineethanesulfonic acid buffer (pH 7.4) was then added up to the required concentration. The different solutions as well as Milli-Q® water were filtered with 0.2-μm FP030/3 filters (Schleicher & Schuell GmbH, Germany). Incubations were carried out at 37 °C for 24 h. Samples were prepared by placing a drop of DNA solution or DNA–compound solution onto mica (Ted Pella, Inc., Redding, CA). After adsorption for 5 min at room temperature, the samples were rinsed for 10 s in a jet of deionized water (18 MΩ cm⁻¹ from a Milli-Q® water purification system) directed onto the surface. The samples were blow-dried with compressed argon and then imaged using AFM. The samples were imaged using a Nanoscope III Multimode AFM (Digital Instrumentals Inc., Santa Barbara, CA) operating in tapping mode in air at a scan rate of 1–3 Hz. The AFM probe was a 125-mm-long monocrystalline silicon cantilever with integrated conical-shaped Si tips (Nanosensors GmbH, Germany) with an average resonance frequency $f_o = 330$ kHz and spring constant $K = 50$ N/m. The cantilever was rectangular and the tip radius given by the supplier was 10 nm, with a cone angle of 35° and high aspect ratio. The images were obtained at room temperature ($T = 23 \pm 2$ °C) and relative humidity was usually lower than 40 % [45].

Viscosity measurements Viscosity experiments were conducted at 25 °C on an automated AND viscometer model SV-10. Stock solutions of each complex were prepared in DMSO/water (4:1) and used immediately after preparation. A 1 mM CT DNA solution was diluted 1:4 with TE buffer. For each complex, increasing amounts of complex stock solution were added to this DNA solution to reach complex/DNA molar ratios in the range 0–2.0. The DMSO amount in the samples never exceeded 2 %. After thermal equilibrium was achieved (15 min), the viscosity of each sample was repeatedly measured. Mean values of five measurements performed at intervals of 1 min were used to evaluate the viscosity of each sample [46].

Cruzipain inhibitory activity Cruzipain was purified to homogeneity from epimastigotes of Tulahuen 2 strain [47]. Cruzipain (2.6 nM) was incubated in 50 mM Tris–HCl (pH 7.6), 150 mM sodium chloride, 100 mM EDTA,

containing 1 M dithiothreitol and inhibitor for 5 min at 37 °C. Then, the fluorogenic substrate Z-phenyl-arginine-7-amido-4-methylcoumarin hydrochloride (Michaelis–Menten constant: $K_M = 3$ μM) was added to give 10 mM substrate. Changes in fluorescence intensity, corresponding to the formation of the hydrolysis product 7-amino-4-methylcoumarin (AMC), were registered for 5 min at excitation and emission wavelengths of 390 and 460 nm, respectively, with a microplate fluorescence reader (FLUOstar* OPTIMA, BMG Labtechnologies). A calibration curve, fluorescence units (FU) vs. AMC (in micromolar), was carried out before each experiment to convert FU into AMC formation (in micromolar). The final assay volume was 200 μL with a DMSO concentration of 20 %. At this concentration, DMSO did not significantly affect the activity of cruzipain. Stock solutions (10 mM) of the ruthenium inhibitors were prepared in DMSO and screened at 10 and 50 μM in duplicate. Controls were performed using the enzyme dissolved in DMSO. The percentage of cruzipain inhibition (CI) was calculated as follows: CI (%) $= (v_i/v_o) \times 100 - 100$, where v_i and v_o correspond to the velocity of AMC formation, [AMC] (in micromolar)/t (in seconds), with and without inhibitor, respectively. E64, trans-epoxysuccinyl-L-leucyl-amido(4-guanidino) butane, was used at 14 nM as a positive control (100 % inhibition) [48].

References

1. Navarro M, Gabbiani G, Messori L, Gambino D (2010) Metal based drugs for malaria, trypanosomiasis and leishmaniasis. Recent achievements and perspectives. Drug Discov Today 15:1070–1077

2. Hotez PJ, Molyneux DH, Fenwick A, Kumaresan J, Ehrlich Sachs S, Sachs JD, Savioli L (2007) Control of neglected tropical diseases. N Engl J Med 357:1018–1027

3. Ribeiro I, Sevcsik AM, Alves F, Diap G, Don R, Harhay MO, Chang S, Pecoul B (2009) New improved treatments for Chagas disease: from the R&D pipeline to the patients. PLoS Negl Trop Dis 3:e484. doi:10.1371/journal.pntd.0000484

4. Urbina J (2003) New chemotherapeutic approaches for the treatment of Chagas disease (American trypanosomiasis). Exp Opin Ther Patents 13:661–669

5. Le Loup G, Pialoux G, Lescure FX (2011) Update in treatment of Chagas disease. Curr Opin Infect Dis 24:428–434

6. Chibale K (2002) Towards broadspectrum antiprotozoal agents. ARKIVOC IX 93–98

7. El-Sayed NM et al (2005) Comparative genomics of trypanosomatid parasitic protozoa. Science 309:404–409

8. Sánchez-Delgado RA, Anzellotti A (2004) Metal complexes as chemotherapeutic agents against tropical diseases: trypanosomiasis, malaria and leishmaniasis. Minirev Med Chem 1:23–30

9. Sánchez-Delgado RA, Anzellotti A, Suárez L (2004) Metal complexes as chemotherapeutic agents against tropical diseases: malaria, trypanosomiasis, and leishmaniasis. In: Sigel H, Sigel A (eds) Metal ions in biological systems, 41: metal ions and their complexes in medication. Marcel Dekker, New York, pp 379–419

10. Magalhães Moreira DR, Lima Leite AC, Ribeiro dos Santos R, Soares MBP (2009) Approaches for the development of new anti-Trypanosoma cruzi agents. Curr Drug Targets 10:212–231

11. Cavalli A, Bolognesi ML (2009) Neglected tropical diseases: multi-target-directed ligands in the search for novel lead candidates against trypanosoma and leishmania. J Med Chem 52:7339–7359

12. Fricker SP, Mosi RM, Cameron BR, Baird I, Zhu Y, Anastassov V, Cox J, Doyle PS, Hansell E, Lau G, Langille J, Olsen M, Qin L, Skerlj R, Wong RSV, Santucci Z, McKerrow JH (2008) Metal compounds for the treatment of parasitic diseases. J Inorg Biochem 102:1839–1845

13. Morphy R, Rankovic Z (2005) Designed multiple ligands. An emerging drug discovery paradigm. J Med Chem 48:6523–6543

14. Otero L, Vieites M, Boiani L, Denicola A, Rigol C, Opazo L, Olea-Azar C, Maya JD, Morello A, Krauth-Siegel RL, Piro OE, Castellano E, González M, Gambino D, Cerecetto H (2006) Novel antitrypanosomal agents based on palladium nitrofurylthiosemicarbazone complexes: DNA and redox metabolism as potential therapeutic targets. J Med Chem 49:3322–3331

15. Vieites M, Otero L, Santos D, Gajardo D, Toloza J, Figueroa R, Norambuena E, Olea-Azar C, Aguirre G, Cerecetto H, González M, Morello A, Maya JD, Garat B, Gambino D (2008) Platinum(II) metal complexes as potential anti-Trypanosoma cruzi agents. J Inorg Biochem 102:1033–1043

16. Vieites M, Otero L, Santos D, Olea-Azar C, Norambuena E, Aguirre G, Cerecetto H, González M, Kemmerling U, Morello A, Maya JD, Gambino D (2009) Platinum-based complexes of bioactive 3-(5-nitrofuryl)acroleine thiosemicarbazones showing anti-Trypanosoma cruzi activity. J Inorg Biochem 103:411–418

17. Pagano M, Demoro B, Toloza J, Boiani L, González M, Cerecetto H, Olea-Azar C, Norambuena E, Gambino D, Otero L (2009) Effect of ruthenium complexation on trypanocidal activity of 5-nitrofuryl containing thiosemicarbazones. Eur J Med Chem 44:4937–4943

18. Gambino D, Otero L (2012) Perspectives on what ruthenium-based compounds could offer in the development of potential antiparasitic drugs. Inorg Chim Acta 393:103–114

19. Demoro B, Sarniguet C, Sánchez-Delgado R, Rossi M, Liebowitz D, Caruso F, Olea-Azar C, Moreno V, Medeiros A, Comini MA, Otero L, Gambino D (2012) New organoruthenium complexes with bioactive thiosemicarbazones as co-ligands: potential anti-trypanosomal agents. Dalton Trans 41:1534–1543

20. Aguirre G, Cerecetto H, González M, Gambino D, Otero L, Olea-Azar C, Rigol C, Denicola A (2004) In vitro activity and mechanism of action against the protozoan parasite Trypanosoma cruzi of 5-nitrofuryl containing thiosemicarbazones. Bioorg Med Chem 12:4885–4893

21. Cazzulo JJ (2002) Proteinases of Trypanosoma cruzi: potential targets for the chemotherapy of Chagas disease. Curr Topics Med Chem 2:1261–1271

22. Greenbaum DC, Mackey Z, Hansell E, Doyle P, Gut J, Caffrey CR, Lehrman J, Rosenthal PJ, McKerrow JH, Chibale K (2004) Synthesis and structure-activity relationships of parasiticidal thiosemicarbazone cysteine protease inhibitors against Plasmodium falciparum, Trypanosoma brucei, and Trypanosoma cruzi. J Med Chem 47:3212–3219

23. Chen H, Parkinson JA, Parsons S, Coxall RA, Gould RO, Sadler PJ (2002) Organometallic ruthenium(II) diamine anticancer complexes: arene-nucleobase stacking and stereospecific hydrogen-bonding in guanine adducts. J Am Chem Soc 124:3064–3082

24. Chen H, Parkinson JA, Morris RE, Sadler PJ (2003) Highly selective binding of organometallic ruthenium ethylenediamine complexes to nucleic acids: novel recognition mechanisms. J Am Chem Soc 125:173–186

25. Caruso F, Rossi M, Benson A, Opazo C, Freedman D, Monti E, Gariboldi MB, Shaulky J, Marchetti F, Pettinari R, Pettinari C (2012) Ruthenium–arene complexes of curcumin: X-ray and density functional theory structure, synthesis, and spectroscopic characterization, in vitro antitumor activity, and DNA docking studies of (p-cymene)Ru(curcuminato)chloro. J Med Chem 55:1072–1081

26. Gambino D, Otero L, Vieites M, Boiani M, González M, Baran EJ, Cerecetto H (2007) Vibrational spectra of palladium 5-nitrofuryl thiosemicarbazone complexes: experimental and theoretical study. Spectrochim Acta A Mol Biomol Spectrosc 68:341–348

27. Therrien B (2009) Functionalised η^6-arene ruthenium complexes. Coord Chem Rev 253:493–519

28. Buettner GR (1987) Spin trapping: ESR parameters of spin adducts. Free Rad Biol Med 3:259–303

29. Moreno SNJ, Schreiber J, Mason RP (1986) Nitrobenzyl radical metabolites from microsomal reduction of nitrobenzyl chlorides. J Biol Chem 261:7811–7815

30. Makino K, Hagiwara T, Murakami A (1991) A mini review: fundamental aspects of spin trapping with DMPO. Radiat Phys Chem 37:657–665

31. Veerapen N, Taylor SA, Walsby CJ, Pinto BM (2006) A mild Pummerer-like reaction of carbohydrate-based selenoethers and thioethers involving linear ozonide acetates as putative intermediates. J Am Chem Soc 128:227–239

32. Otero L, Folch C, Barriga G, Rigol C, Opazo L, Vieites M, Gambino D, Cerecetto H, Norambuena E, Olea-Azar C (2008) ESR, electrochemical and reactivity studies of antitrypanosomal palladium thiosemicarbazone complexes. Spectrochim Acta Part A Mol Biomol Spect 70:519–523

33. Onoa GB, Cervantes G, Moreno V, Prieto MJ (1998) Study of the interaction of DNA with cisplatin and other Pd(II) and Pt(II) complexes by atomic force microscopy. Nucleic Acids Res 26:1473–1480

34. Vieites M, Smircich P, Pagano M, Otero L, Luane Fischer F, Terenzi H, Prieto MJ, Moreno V, Garat B, Gambino D (2011) DNA as molecular target of analogous palladium and platinum anti-Trypanosoma cruzi compounds: a comparative study. J Inorg Biochem 105:1704–1711

35. Satyanarayana S, Dabrowiak JC, Chaires JB (1992) Neither delta- nor lambda-tris(phenanthroline)ruthenium(II) binds to DNA by classical intercalation. Biochemistry 31:9319–9324

36. Satyanaryana S, Dabrowiak JC, Chaires JB (1993) Tris(phenanthroline)ruthenium(II) enantiomer interactions with DNA: mode and specificity of binding. Biochemistry 32:2573–2584

37. Bai G, Dong D, Lu Y, Wang K, Jin L, Gao L (2004) A comparative study of the interaction of two structurally analogue ruthenium(II) complexes with DNA. J Inorg Biochem 98:2011–2015

38. Novakova O, Chen H, Vrana O, Rodger A, Sadler PJ, Brabec V (2003) DNA interactions of monofunctional organometallic ruthenium(II) antitumor complexes in cell-free media. Biochemistry 42:11544–11554

39. Gill MR, Thomas JA (2012) Ruthenium(II) polypyridyl complexes and DNA—from structural probes to cellular imaging and therapeutics. Chem Soc Rev 41:3179–3192

40. Sheldrick GM (2008) A short history of SHELX. Acta Crystallogr A64:112–122

41. Maya JD, Morello A, Repetto Y, Tellez R, Rodriguez A, Zelada U, Puebla P, Bontá M, Bollo S, San Feliciano A (2000) Effects of 3-chloro-phenyl-1,4-dihydropyridine derivatives on Trypanosoma cruzi epimastigotes. Comp Biochem Physiol C Toxicol Pharmacol 125:103–109

42. Cuellar MA, Salas C, Cortés MJ, Morello A, Maya JD, Preite MD (2003) Synthesis and in vitro trypanocide activity of several polycyclic drimane-quinone derivatives. Bioorg Med Chem 11:2489–2497

43. Muelas-Serrano S, Nogal-Ruiz JJ, Gómez-Barrio A (2000) Setting a colorimetric method to determine the viability of Trypanosoma cruzi epimastigotes. Parasitol Res 86:999–1002

44. Faundez M, Pino L, Letelier P, Ortiz C, López R, Seguel C, Ferreira J, Pavani M, Morello A, Maya JD (2005) Buthionine sulfoximine increases the toxicity of nifurtimox and benznidazole to Trypanosoma cruzi. Antimicrob Agents Chemother 49:126–130

45. Benítez J, Guggeri L, Tomaz I, Costa Pessoa J, Moreno V, Lorenzo J, Avilés FX, Garat B, Gambino D (2009) A novel vanadyl complex with a polypyridyl DNA intercalator as ligand: a potential anti-protozoa and anti-tumor agent. J Inorg Biochem 103:1386–1394

46. Zhang G, Guo J, Pan J, Chen X, Wang J (2009) Spectroscopic studies on the interaction of morin–Eu(III) complex with calf thymus DNA. J Mol Structure 923:114–119

47. Parussini F, García M, Mucci J, Agüero F, Sánchez D, Hellman U, Åslund L, Cazzulo JJ (2003) Characterization of a lysosomal serine carboxypeptidase from Trypanosoma cruzi. Mol Biochem Parasitol 13:11–23

48. Siles R, Chen S, Zhou M, Pinney K, Trawick M (2006) Design, synthesis, and biochemical evaluation of novel cruzain inhibitors with potential application in the treatment of Chagas' disease. Bioorg Med Chem Lett 16:4405–4409